Geo-spatial Information Science

ISSN: (Print) (Online) Journal homepage: https://www.tandfonline.com/loi/tgsi20

EFFC-Net: lightweight fully convolutional neural networks in remote sensing disaster images

Jianye Yuan, Xin Ma, Zhentong Zhang, Qiang Xu, Ge Han, Song Li, Wei Gong, Fangyuan Liu & Xin Cai

To cite this article: Jianye Yuan, Xin Ma, Zhentong Zhang, Qiang Xu, Ge Han, Song Li, Wei Gong, Fangyuan Liu & Xin Cai (17 May 2023): EFFC-Net: lightweight fully convolutional neural networks in remote sensing disaster images, Geo-spatial Information Science, DOI: 10.1080/10095020.2023.2183145

To link to this article: https://doi.org/10.1080/10095020.2023.2183145

Published online: 17 May 2023.

GEO-SPATIAL INFORMATION SCIENCE
https://doi.org/10.1080/10095020.2023.2183145

Taylor & Francis
Taylor & Francis Group

EFFC-Net: lightweight fully convolutional neural networks in remote sensing disaster images

Jianye Yuan[a], Xin Ma[b], Zhentong Zhang[c], Qiang Xu[d], Ge Han[e], Song Li[a], Wei Gong[a], Fangyuan Liu[f] and Xin Cai[g]

[a]School of Electronic Information, Wuhan University, Wuhan, China; [b]State Key Laboratory of Information Engineering in Surveying, Mapping, and Remote Sensing Wuhan University, Wuhan, China; [c]School of Cyber Science and Engineering, Southeast University, Nanjing, China; [d]Department of Electrical Engineering, and Center for Intelligent Multidimensional Data Analysis, City University of Hong Kong, Hong Kong, China; [e]School of Remote Sensing and Information Engineering, Wuhan University, Wuhan, China; [f]The Second Clinical Medical College, Jinan University, Shenzhen, China; [g]School of Electrical Engineering, Xinjiang University, Urumqi, China

ABSTRACT

Continuous development of remote sensing technology can rapidly and accurately extract secondary disaster information, such as the area of various disasters. However, in the extraction process, some disasters should be initially classified and identified. In view of this concept, a lightweight fully Convolutional Neural Network (CNN) model Earthquake – Flood–Fire – Cyclone (EFFC)-Net is proposed. Two modules, EFFC_Block and EFFC_Tran_Block, which are used for feature extraction and feature transformation, respectively, are introduced. The EFFC-Net network model is reconstructed through the EFFC_Block and EFFC_Tran_Block modules. Subsequently, EFFC-Net is compared with CNN and transformer models. Results show that the EFFC-Net network model performs effectively in precision, recall, F1_score, and parameters, outperforming the more advanced CNN and transformer models. Moreover, the test time of the Cifar_10 and Cifar_100 datasets was compared, and the results indicate that the EFFC-Net algorithm has the shortest running time and achieves the lightweight goal. Therefore, the EFFC-Net lightweight fully CNN has high disaster classification application value and good portability.

ARTICLE HISTORY
Received 27 July 2022
Accepted 17 February 2023

KEYWORDS
EFFC-Net; CNN; transformer; remote sensing image; fully convolutional neural network

1. Introduction

The United Nations defines a disaster as a factor that causes damage to human life and property in the natural environment (Ogie, Rho, and Clarke 2018). In the process of disaster prediction and early warning, specific classification preprocessing for some disasters should be carried out. Traditional disaster relief pre-classifies disasters by statistical methods, which are inefficient and require high data volume. At this stage, some researchers combine modern computer technology and satellite remote sensing technology to study disaster relief and use machine learning methods to deal with disasters. For example, Li et al. (2021) used Softmax regression model to predict the loss degree of earthquake disasters; (Wu et al. 2022) proposed the use of XGBoost to predict railway construction accident disasters to improve the prediction effect; Song and Park (2019) proposed a natural disaster loss prediction formula under the condition considering the economic indicators of each country and proved the effectiveness of the modified formula through experiments. In Li et al. (2022), the authors discuss the feasibility of micro-current technology for predicting coal and rock dynamic disasters; Chai et al. (2021) improved the response speed of power grid emergency material deployment based on the power grid emergency repair efficiency. A method combining case reasoning and deep learning is proposed to classify emergency materials under the condition of power grid meteorological disasters. In these research results, some disasters are predicted, and a method is proposed to verify the prediction of some disasters and assess the degree of loss to provide better help for subsequent disaster reconstruction. These methods deal with a single disaster category, and the accuracy of the processing results is low. Therefore, in response to these problems, a disaster classification method based on remote sensing images is proposed.

In addition to the importance of classification accuracy, the time consumed by the classification is relevant. Thus, the speed is also a focus of our research, paving the way for subsequent porting to development boards, such as embedded devices. The disaster category can be rapidly extracted using the classification technology of regional images, avoiding the use of human and material resources and further reducing the problems of inaccurate disaster prediction and low efficiency. At the same time, in the field of deep learning, the best current research performed is CNN and the transformer model proposed in recent years.

CONTACT Xin Ma maxin@whu.edu.cn

The proposal of CNN creates a precedent for image processing technology, and that of the transformer solves various problems on the short board of CNN. This approach introduces artificial intelligence, specifically in the field of disaster image classification.

At present, a fixed and unified method for the classification of disaster categories is unavailable in the scientific community, and large differences exist between different disasters. According to the United Nations regulations, the disasters can be categorized into natural disasters, meteorological disasters, biological disasters, and astronomical disasters, among which natural disasters include volcanoes, earthquakes, tsunamis, landslides, and mudslides; meteorological disasters include typhoons, rainstorms, floods, droughts, sandstorms, and smog; biological disasters include pests, epidemics, rodents, locusts, species invasion, and red tides; astronomical disasters include meteors and cosmic rays. For this study, we selected four types of natural disasters with greatest impact on people's lives and properties, namely, earthquake, flood, fire, and cyclone, and proposed a classification model suitable for application to the four types of disasters by combining the influence of remote sensing – EFFC.

The main contributions of this paper are as follows:

(1) Two Convolution (ConV) blocks were proposed, namely, EFFC_Block and EFFC_Tran_Block, which are used for feature extraction and feature conversion, respectively;
(2) A new fully convolutional disaster classification network EFFC-Net was proposed;
(3) We have experimentally demonstrated the effectiveness of the EFFC-Net network for disaster classification tasks. The EFFC-Net network has better results, higher accuracy, lower computation, and number of parameters. It also performs better on public datasets and can be used for other classification tasks.

2. Related work

2.1. CNN model

With the continuous development and maturity of deep learning, its classification effect gradually exceeds that of human visual classification, and the classification accuracy is also improved. The emergence of AlexNet (Alom et al. 2018) re-exposed CNN to scientists; ResNet (Wen, Li, and Gao 2020) solved the phenomenon of gradient disappearance and explosion; the spatial and channel attention mechanism proposed by SENet (Li et al. 2021) further improved the model effect and provided ideas for the subsequent transformer proposal; EfficientNet (Marques et al. 2020) integrated the three-channel model extension, which greatly reduces the Floating Point Operations (FLOPs) and number of Parameters (Params) of the model; RegNet (Dong et al. 2021) used neural architecture search technology to further adjust the specific Params and apply it to the field of autonomous driving. Although more methods of classification models are available and the effects are improving, the network model structure still includes Input, Hidden, and Output. The simplest CNN structure is shown in Figure 1.

2.2. Transformer

Many new models have been proposed with the continuous development of attention mechanisms. In 2017, the transformer was used for Natural Language Processing (NLP) tasks and achieved satisfactory results, and then it was applied to the image classification task. The transformer model structure has good experimental results in many fields; thus, it has received considerable research attention. For example, Bert (Devlin et al. 2018; Zhang et al. 2023), DETR (Gao et al. 2021), iGPT (Nakajima et al. 2019), ViT (Dosovitskiy et al. 2020), IPT (Chen et al. 2021), and ViT Variants (Eweida et al. 2021) achieved good results on image classification tasks.

As shown in Figure 2, the transformer is mainly composed of the encoder and the decoder in the attention mechanism. The structure of each encoder and decoder is the same except for some parameter settings. Therefore, the encoder and the decoder generally have a one-to-one correspondence.

3. Method

This research builds the neural network from scratch and redesigns a disaster classification network structure. Its architecture includes ConV layer, BatchNorm and LazyBatchNorm, ReLU6 (Zou et al. 2020) activation function, Max pooling, and Average pooling layer. A ConV layer can have multiple different ConV kernels, but each ConV kernel corresponds to a new feature map after filtering. BatchNorm and LazyBatchNorm are mainly

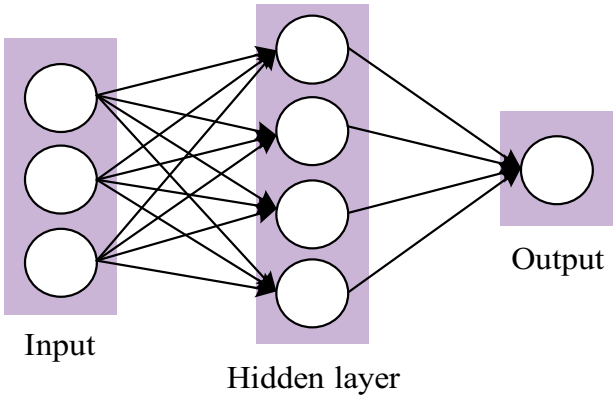

Figure 1. Structure of the simplest CNN model.

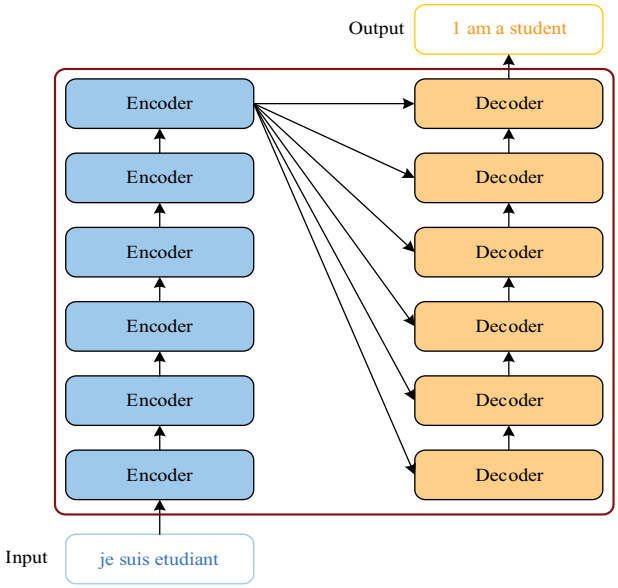

Figure 2. Transformer model structure diagram.

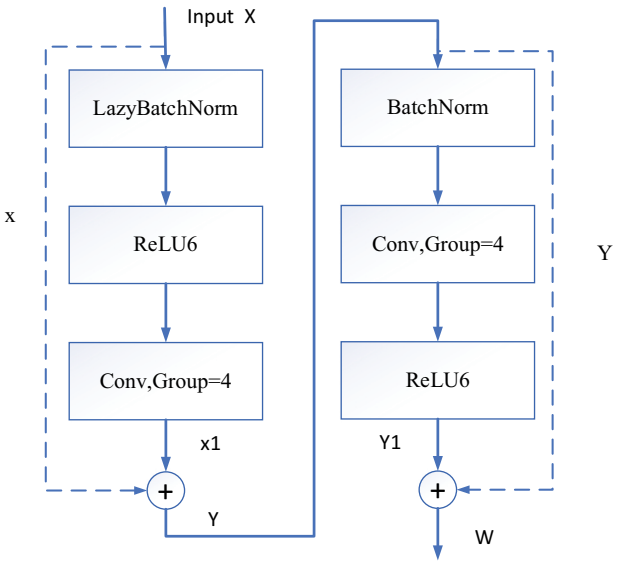

Figure 3. Effc_block structure diagram.

used to speed up the training and the convergence of the network and prevent the network from overfitting. The activation function is mainly used to increase the nonlinearity of the network and improve its expressiveness. Common activation functions are Sigmoid (Batou 2019), tanh (Rabie and Ahmed 2021), Relu (Agarap 2018), Leaky ReLU (Zou et al. 2020), Exponential Linear Units (ELU) (Arroyo-Fernández et al. 2018), MaxOut (Zhao et al. 2018), and ReLU6. The ReLU6 activation function is shown in Formula 1, where f is the input feature value, and the output feature value is up to 6. Therefore, the activation function used in this study is ReLU6, which avoids the occurrence of gradient explosion in the ReLU activation function. The pooling layer is also called the downsampling layer; computation is reduced by downsampling. The main function is to prevent the network from overfitting during the network calculation process and improve the generalization ability of the network. General pooling, average pooling, and max pooling are common pooling layers, among which the two latter layers were used in this study.

$$\mathrm{ReLU6} = \min(\max(f, 0), 6) \tag{1}$$

3.1. Algorithm structure

The research proposes two blocks, namely, EFFC_Block and EFFC_Tran_Block, which play the role of feature extraction and feature transformation. Through the EFFC_Block, EFFC_Tran_Block, and ConV layer, the activation function and maximum pooling layer constitute an EFFC-Net disaster classification model.

3.1.1. Effc_block

As shown in Figure 3, the EFFC_Block consists of LazyBatchNorm, ReLU6, and depthwise ConV (Tan et al. 2019), where the number of groups is set to 4, and the Params are connected through shortcut connection *X*. After the BatchNorm, the deep ConV and ReLU6 with a group number of 4 are still used, and the shortcut connection *Y* is used to connect the Params again; the final output value is *W*. By using two shortcut connections, the intercommunication between data is greatly strengthened, and the information in the upper layer can be integrated with the deeper information, thereby improving the feature extraction efficiency of the network.

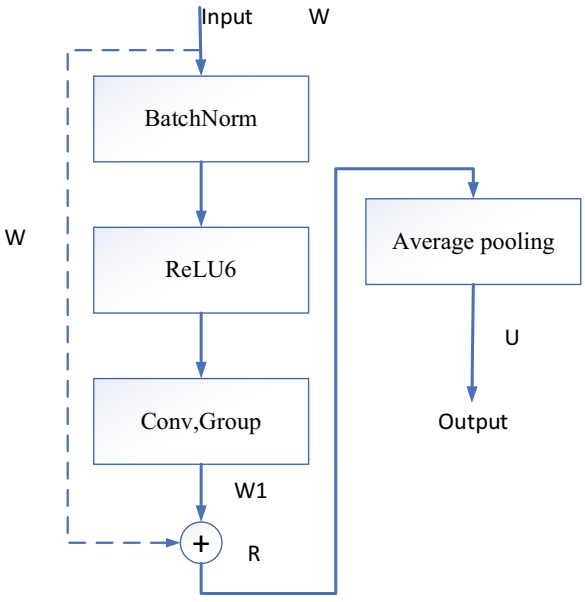

Figure 4. Effc_tran_block structure diagram.

3.1.2. Effc_tran_block

As shown in Figure 4, the EFFC_Block consists of BatchNorm, ReLU6, and depthwise ConV, where group ConV (Zhang et al. 2018) is set to the same number of output channels as the ConV layer. This method not only improves the feature extraction ability of the network but also greatly reduces the complexity of the algorithm. The role of the shortcut connection W is to perform feature fusion on the network. Subsequently, the output value U of the EFFC_Block is obtained through average pooling.

We propose a new disaster classification network, and the EFFC-Net network visualization model is shown in Figure 5. Initially, four types of disaster image information are input. The ConV layer should include the following: the number of input channels is 3, the number of output channels is 64, the ConV kernel is 7×7, the stride is 2, and the padding is 3. Then, the BatchNorm layer and the Max Pool layer should include the following: Max Pool ConV kernel is 3×3, stride is 2, padding is 1, and dilation is 1. Subsequently, the output feature map information is used for feature extraction and feature transformation on the EFFC_Block and EFFC_Tran_Block modules. BatchNorm and ReLU6 do not change the input and output values of the network. Their function is to increase the nonlinearity of the network and prevent the network from overfitting. Therefore, the research does not visualize BatchNorm and ReLU6 for the objectivity of Figure 5, but the EFFFH_Block and EFFC_Tran_Block modules are shown in Figures 3 and 4, respectively, and will not be described here.

The EFFC_Block module has two ConV layers, each of which has the following parameters: the number of input channels is 64, the number of output channels is 128, the ConV kernel is 1×1, the stride is 1, the padding is 1, and the group is depthwise with four ConV. After passing through the EFFC_Tran_Block module, its

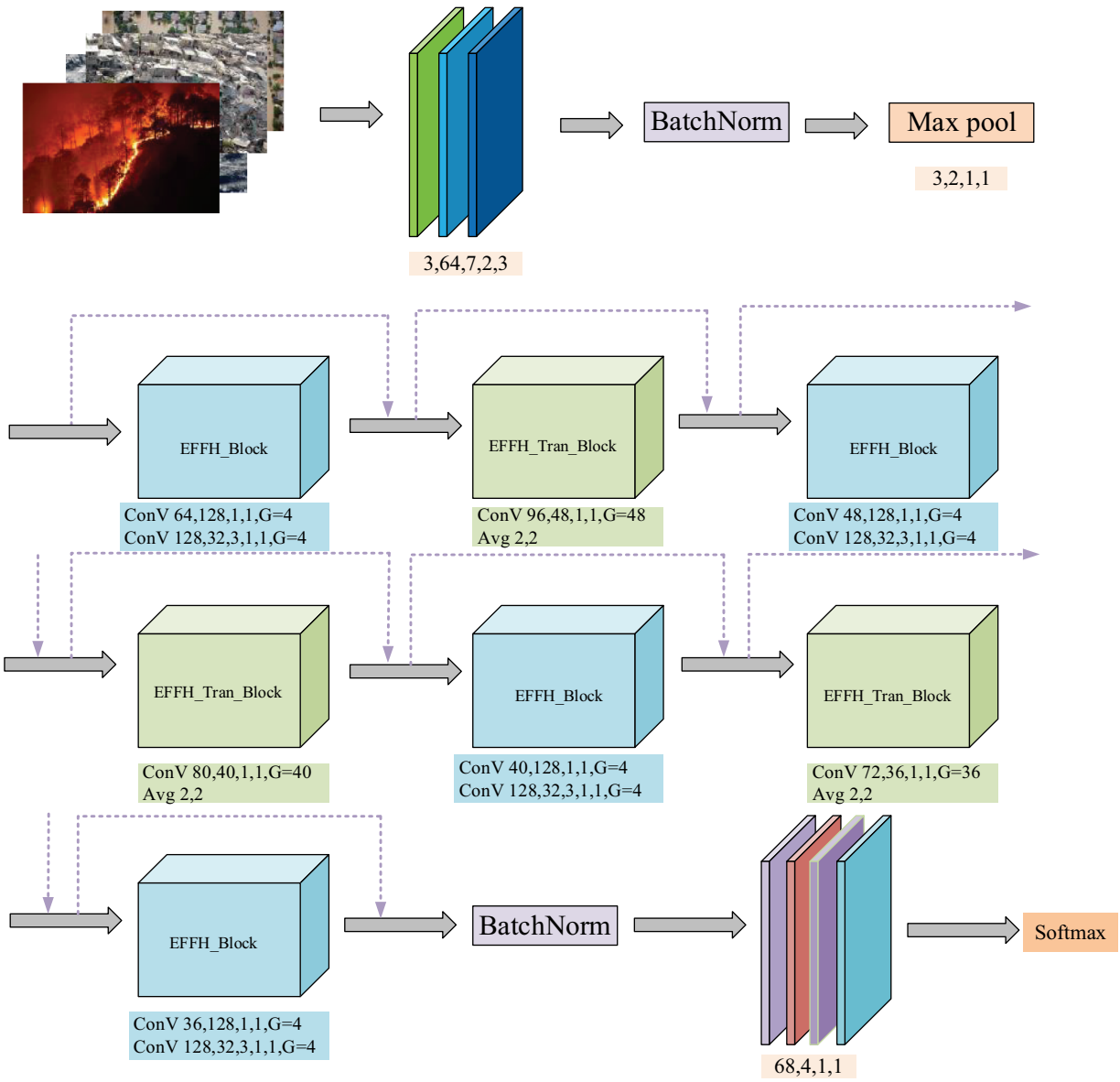

Figure 5. EFFC-Net network structure diagram.

specific parameters become as follows: the number of input channels is 96, the number of output channels is 48, the size of the ConV kernel is 1×1, the stride is 1, and the group of depthwise ConV is the same as the number of output channels, which is 48 here. In addition, the avgpool layer has a kernel size of 2×2 and a stride of 2. The EFFC-Net networks visualized according to the above principles are connected in sequence, and finally the information of the upper layer is transmitted to the information of the next layer through intensive shortcut connection, thereby improving the feature extraction ability of the network. Figure 5 shows that the EFFC-Net network contains four EFFC_Blocks and three EFFC_Tran_Blocks. Each of the EFFC_Block and EFFC_Tran_Block is set at intervals and connected through a dense shortcut connection. Finally, the feature output is carried out through the last layer of the ConV layer, and the output value is the maximum probability value of the four types of disaster images. The EFFC-Net network structure diagram in Figure 5 only shows the shortcut connections between the adjacent layers. In fact, the network in the research uses dense shortcut connections. Each layer is connected to the next layer to further increase the algorithm efficiency. In the figure, ConV is used to represent the ConV layer.

4. Experimental sessions

4.1. Lab environment

The experiments in the research were carried out on a 64-bit operating system, Ubuntu 20.04.3 LTS, and NVIDIA graphics card 3090 24 G video memory, and the dataset from this experiment is obtained from the "Kaggle" competition (AswinGopinathan 2021) and State Key Laboratory of Information Engineering in Surveying, Mapping, and Remote Sensing for Surveying and Mapping. A total of 9792 pictures, 7791 pictures in the train datasets and 2001 pictures in the test datasets. The number of images for each type of disaster data is shown in Table 1. All images have a horizontal resolution of 96 dpi, a vertical resolution of 96 dpi, and a bit depth of 24. Considering the performance of the graphics card, the batch size of each training input image is fixed to 16, the optimizer is Stochastic Gradient Descent (SGD) (Garcia et al. 2021; Cai and Chen 2022), the initial learning rate is 0.01, the weight decay is 0.0004, the step size is 5, and cross is used for Cross Entropy Loss (CEL) (Jamin and Humeau-Heurtier 2019).

Table 1. Number of images of each category in the disaster dataset.

	Train	Test	Total
Cyclone	744	185	929
Earthquake	1092	273	1365
Flood	3004	806	3810
Wildfire	2951	737	3688
Total	7791	2001	9792

4.2. Evaluation indicators

The image classification evaluation indicators selected in the research are confusion matrix (Luque et al. 2019), precision, accuracy change curve, loss function change curve, recall, and Receiver Operating Characteristic (ROC) curve. The confusion matrix includes the prediction result and the actual result, and a table is made in each category. The predicted results of each category and the actual results of the statistical data table are recorded. For a k-order classification network, the confusion matrix is a $k \times k$ tabular matrix. As shown in Table 2, when the predicted value is the same as the actual value, the predicted result is true; otherwise, it is false.

The samples predicted to be positive by the precision reaction are true positive samples, and the calculation method is shown in Formula 2. Recall indicates the number of positive samples accurately predicted, and the calculation method is shown in Formula 3. F1_score is used to avoid considering precision and recall as the only evaluation indicators. The F1_score obtains the optimal network effect by balancing precision and recall. The calculation method is shown in Formula 4.

$$\text{Precision} = \frac{\text{TP}}{\text{TP} + \text{FP}} \tag{2}$$

$$\text{Recall} = \frac{\text{TP}}{\text{TP} + \text{FN}} \tag{3}$$

$$\text{F1\_score} = \frac{2 \times \text{Precision} \times \text{Recall}}{\text{Precision} + \text{Recall}} \tag{4}$$

Among them, the research uses True Positive(TP) instead of prediction is positive and actuality is positive; False Positive (FP) instead of prediction is positive and actuality is negative; False Negative (FN)

Table 2. Confusion matrix for four types of disasters.

		Real category			
		Cyclone	Earthquake	Flood	Wildfire
Prediction category	Cyclone	**True**	False	False	False
	Earthquake	False	**True**	False	False
	Flood	False	False	**True**	False
	Wildfire	False	False	False	**True**

instead of prediction is negative and actuality is negative; True Negative (TN) instead of prediction is negative and actuality is positive.

The running time evaluation index used by the research is expressed by time, as shown in formula 5, where T_{start} is used to represent the start time, T_{end} is used to represent the end time, T_{test} is used to represent the test time, and the difference is the running time of the research algorithm, which is recorded as all test datasets in the research testing time.

$$T_{test} = T_{end} - T_{start} \tag{5}$$

Loss function, also known as cost function or error function, is used to evaluate the difference between the predicted value and the actual value. The smaller loss function value indicates that the predicted value x is closer to the actual value y. The common loss functions are mean absolute error (MAE) loss (Camero, Toutouh, and Alba 2019), mean squared error (MSE) loss (Lucas et al. 2019), Huber loss (Gupta, Hazarika, and Berlin 2020), Log–Cosh loss (Xu et al. 2020), quantile loss (Yang and Dong 2019), hinge loss (Rodríguez 2019), and focal loss (Acharya et al. 2019). The loss function used by the research is CEL, and its calculation method is shown in Formula 6.

$$C = -\frac{1}{n}\sum_{k=0}^{n}[x\ln y + (1-x)\ln(1-y)] \tag{6}$$

The role of the optimizer is to set each parameter in the loss function to be more in line with the network training parameters during the backpropagation process of the network; thus, the value of the loss function continuously approaches the global minimum. The common optimizers are gradient descent (GD) (Du et al. 2019), Batch Gradient Descent (BGD) (Chen and Shi 2019), SGD, Nesterov (Muehlebach and Jordan 2019), AdaGrad (Ward et al. 2019), and Adam (Zhuang et al. 2020). The research uses the optimizers SGD, Loss, and gradient value, which are calculated for each sample value, and then updated. The formula for calculating the output value θ after SGD is updated is shown in Formula 7.

$$\theta = \theta - \alpha \cdot \quad {}_{\theta}\tau\left(\theta; x^{i}; y^{i}\right) \tag{7}$$

4.3. Comparison of CNN and transformer model data

The EFFC-Net, CNN, and transformer algorithms are compared to verify the performance of the proposed algorithm EFFC-Net in terms of disaster classification. As shown in Table 3, the comparison of CNN's ResNet50, Resnext101, Squeezenet1_0 (Lee et al. 2019), Mnasnet0_5 (Tan et al. 2019), Efficientnet_b5 (Marques et al. 2020), Nasnet (Qin and Wang 2019), Skresnet34 (Zhang and Zhang 2022), and Eca_vovnet39b (Lee et al. 2019) algorithms indicated that Mnasnet0_5 is unsuitable when applied to disaster classification tasks. The precision is only 0.613; thus, Mnasnet0_5 is unsuitable for disaster classification tasks. Compared with other precision results, EFFC-Net performs normally with slight difference. In terms of recall and F1_score, the overall performance of EFFC-Net is better than that of other algorithms, and the effect is similar to Eca_vovnet39b. However, in terms of Params, the EFFC-Net is 6500 times smaller than Eca_vovnet39b, and the effect is evidently better than Eca_vovnet39b. Therefore, the research's EFFC-Net is more suitable for disaster classification tasks than CNN network.

Table 3 shows the comparison of EFFC-Net with the transformer's T2TViT (Zhao et al. 2022), Twins-SVT (Chu et al. 2021), RegionViT (Chen et al. 2021), CrossFormer (Wang et al. 2021), and NesT (Liu et al. 2021) networks. Twins-SVT and CrossFormer networks have poor performance in various indicators and are unsuitable for disaster classification tasks. For the precision, EFFC-Net outperforms T2TViT and RegionViT network, and the effect is similar to NesT; EFFC-Net outperforms T2TViT, RegionViT, and NesT in terms of recall rate. Moreover, in terms of Params, NesT is the best transformer network, but still 500 times larger than the EFFC-Net network. Therefore, the results indicate that the overall performance of EFFC-Net is better than that of the

Table 3. Comparison of EFFC-Net with CNN and transformer data.

Type	Model	Precision	Recall	F1_score	Params(M)
CNN	ResNet50(2016)	0.899	0.907	0.902	376.83
	Resnext101(2017)	0.903	0.900	0.900	1104.03
	Squeezenet1_0(2016)	0.851	0.867	0.857	92.61
	Mnasnet0_5(2018)	0.613	0.478	0.482	73.58
	Efficientnet_b5(2019)	0.899	0.920	0.909	731.89
	Nasnet(2019)	0.905	0.924	0.913	1518.16
	Skresnet34(2020)	0.909	0.914	0.911	264.26
	Eca_vovnet39b(2020)	0.917	0.938	0.927	324.70
Transformer	T2TViT(2021)	0.892	0.913	0.901	514.93
	Twins-SVT(2021)	0.023	0.250	0.042	1379.04
	RegionViT(2021)	0.888	0.906	0.896	8354.54
	CrossFormer(2021)	0.023	0.250	0.042	380.12
	NesT(2021)	0.907	0.928	0.916	252.96
Ours	**EFFC-Net**	**0.904**	**0.932**	**0.917**	**0.05**

transformer network in the disaster classification task. Therefore, the proposed EFFC-Net network is suitable for application in disaster classification tasks.

4.4. EFFC-Net data visualization

The researcher draws the accuracy and loss change curves of the EFFC-Net disaster classification network to further verify the reliability of the data in Table 3. Figures 6 and 7 show that the network tends to converge after 100 training iterations; thus, the epoch is set to 100. Figure 6 shows that as the number of iterations continues to increase, the accuracy of the network continues to improve. The accuracy of the training set is more stable than that of the validation set, and the curve accuracy does not change after 90 iterations. In addition, Figure 7 shows that the loss value continuously decreases slowly, and the loss stability of the training set is better than that of validation one. To this end, the effectiveness of the proposed EFFC-Net disaster classification network is further verified.

The ROC curve shows the actual category and predicted probability curve of the sample. At the same time, the Area Under Curve (AUC) is positively correlated with the ROC curve. AUC represents the area of the curve and is a performance measure for image classification problems under various threshold settings. Therefore, the higher AUC value indicates the better classification effect. Figure 8 shows that the AUC value becomes closer to 1 during iteration. Thus, the EFFC-Net algorithm becomes better. In addition, Figure 9 shows that the EFFC-Net accurately identified the largest number of floods, followed by fire, earthquake, and cyclone. Therefore, the EFFC-Net is suitable for application in disaster classification tasks.

Figure 10 shows a histogram of the three evaluation metrics of precision, recall, and F1_score on the cyclone, earthquake, flood, and fire categories of the EFFC-Net. The histogram shows that the three evaluation indicators of the EFFC-Net are above 85%, and the average is approximately 90%, without abnormal phenomenon. Therefore, the proposed EFFC-Net has good stability and high-cost performance for the four types of disaster identification and is suitable for disaster classification tasks.

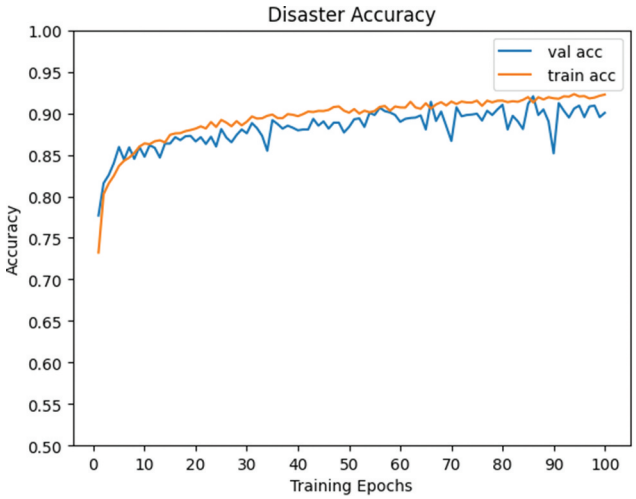

Figure 6. EFFC-Net network accuracy's variation curve.

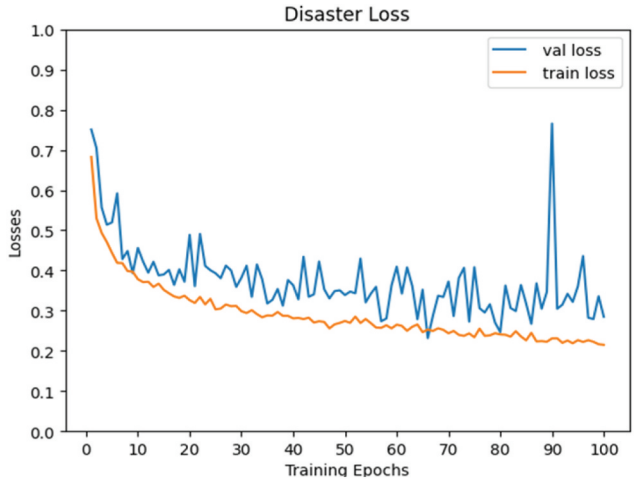

Figure 7. EFFC-Net network loss' variation curve.

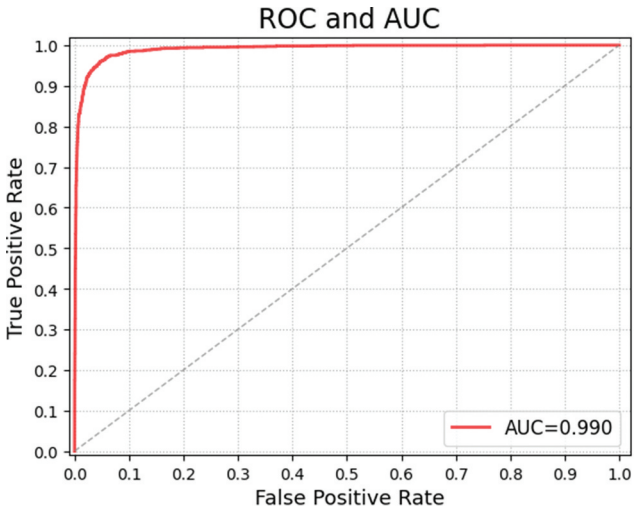

Figure 8. EFFC-Net network's ROC and AUC change curve.

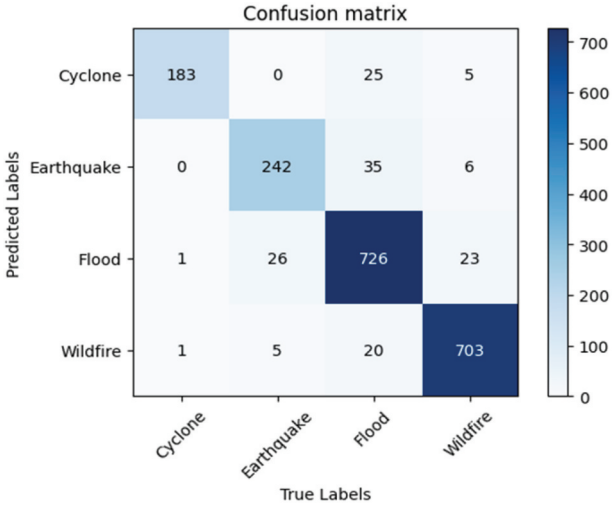

Figure 9. EFFC-Net network's confusion matrix change curve.

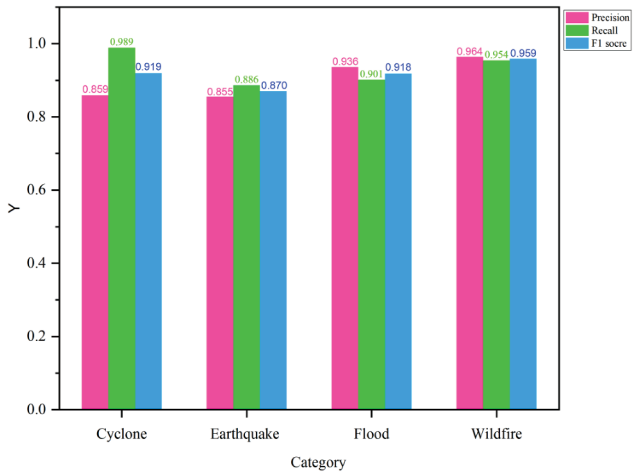

Figure 10. Data of EFFC-Net network on various categories.

4.5. Public datasets

Aside from other performance, the model with the smallest Params on the above-mentioned comparison algorithms is selected, as well as two algorithms with the smallest Params from CNN and transformer. Moreover, the number of iteration cycles is set to 80, 120, 160, and 200 for the experiments.

Table 4. Comparison of running time of algorithms in Cifar_10 and Cifar_100.

Type	Model	Epoch	Total time(s)	Single image test(s)
Cifar_10	**EFFC-Net**	80	**6230**	**3.11**
	Mnasnet0_5		7519	3.76
	squeezenet1_0		6839	3.42
	EFFC-Net	120	**9446**	**4.72**
	Mnasnet0_5		11,233	5.61
	squeezenet1_0		10,259	5.13
	EFFC-Net	160	**12,525**	**6.26**
	Mnasnet0_5		14,946	7.47
	squeezenet1_0		13,729	6.86
	EFFC-Net	200	**15,637**	**7.81**
	Mnasnet0_5		18,838	9.41
	squeezenet1_0		17,601	8.80
Cifar_100	**EFFC-Net**	80	**6503**	**3.25**
	NesT		28,602	14.30
	CrossFormer		48,995	24.49
	EFFC-Net	120	**9711**	**4.85**
	NesT		41,871	20.93
	CrossFormer		74,546	37.25
	EFFC-Net	160	**12,983**	**6.49**
	NesT		57,134	28.55
	CrossFormer		104,293	52.12
	EFFC-Net	200	**16,146**	**8.07**
	NesT		71,585	35.77
	CrossFormer		125,045	62.50

The effect of the algorithm on two public datasets, Cifar_10 (Recht et al. 2018) and Cifar_100 (Singla et al. 2021), in terms of running time, is determined to further verify the advantages of the proposed algorithm, as shown in Table 4. Table 4 shows the comparison between EFFC-Net with Mnasnet0_5 and squeezenet1_0, indicating that at 80, 120, 160, or 200 iterations, the image classification and recognition time of squeezenet1_0 is less than that of Mnasnet0_5, and that of EFFC-Net is less than that of squeezenet1_0. The research algorithm EFFC-Net still maintains the fastest classification speed and the shortest recognition time. In the single test set classification process, the time of EFFC-Net is approximately 1 s faster than that of squeezenet1_0 and 2 s faster than Mnasnet0_5. Therefore, EFFC-Net achieves the lightweight goal on the Cifar_10 dataset.

Subsequently, the EFFC-Net is experimentally compared with NesT and CrossFormer algorithms on the Cifar_100 dataset. Table 4 shows that the classification and recognition time of EFFC-Net algorithm is still the shortest, and it is more evident than Cifar_10. For single image classification, the classification and recognition time of EFFC-Net is only 1/4–1/5 of that of NesT, and approximately 1/8 of that of CrossFormer. Therefore, EFFC-Net achieves the goal of lightweight and has good portability.

5. Conclusions

With the continuous occurrence of natural disasters, responding to and preventing disasters in a timely manner have become increasingly important. In disaster prevention, the category of the disaster should be initially determined. Thus, a lightweight fully CNN model EFFC-Net is proposed to deal with the disaster classification task. The classification of four types of disasters, namely, cyclone, earthquake, flood, and wildfire, is mainly studied. Initially, the EFFC_Block and EFFC_Tran_Block modules are proposed, and the EFFC-Net disaster classification model is composed of the EFFC_Block and EFFC_Tran_Block modules. The comparison with the CNN and transformer networks on the disaster dataset indicates that the proposed EFFC-Net not only has low Params but also has a high classification and recognition accuracy. Finally, this study compared the running time on the Cifar_10 and Cifar_100 datasets and found that the running time of EFFC-Net is still the shortest. Therefore, the proposed EFFC-Net can not only be applied to disaster classification tasks but also to other classification tasks because it has good portability.

Disclosure statement

No potential conflict of interest was reported by the authors.

Funding

This work was supported by the National Natural Science Foundation of China (Grant No. 42171464, 41971283, 41827801), The Key Research and Development Project of Hubei Province (2022BCA057, 2021BCA216), the National Key Research and Development Program of China (2017YFC0212600), A pre-research project (D040107), Wuhan University Specific Fund for Major School-level Internationalization Initiatives, and the LIESMARS Special Research Funding.

Notes on contributors

Jianye Yuan is a PhD student in Wuhan University, with research interests in deep learning, disaster forecasting, and remote sensing imagery.

Xin Ma is an associate researcher at Wuhan University, with research interests in deep learning and atmospheric environment.

Zhentong Zhang is a PhD student in Southeast University, with main research areas in deep learning and machine learning.

Qiang Xu *is a* postdoctoral fellow at City University of Hong Kong, with main research directions in deep learning and machine learning.

Ge Han is an associate professor at Wuhan University, with research interests in deep learning and atmospheric remote sensing.

Song Li is a professor at Wuhan University, with main research areas in deep learning and atmospheric remote sensing.

Wei Gong is a professor at Wuhan University, with main research directions in deep learning and atmospheric remote sensing.

Fangyuan Liu is a master's student in Jinan University, with main research directions in deep learning and machine learning.

Xin Cai is a lecturer at Xinjiang University, with research interests in deep learning and machine learning.

ORCID

Jianye Yuan http://orcid.org/0000-0002-9347-092X
Xin Ma http://orcid.org/0000-0002-0969-2838

Data availability statement

The dataset for this experiment came from the Kaggle competition and State Key Laboratory of Information Engineering in Surveying, Mapping, and Remote Sensing for Surveying and Mapping. Among them, the data URL link on the Kaggle competition is https://www.kaggle.com/aswin1871/cyclonewildfireflood-and-earthquake, State Key Laboratory of Information Engineering in Surveying, Mapping, and Remote Sensing for Surveying and Mapping, Wuhan university.

References

Acharya, U. R., Y. Hagiwara, S. N. Deshpande, S. Suren, J. E. W. Koh, S. L. Oh, N. Arunkumar, E. J. Ciaccio, and C. M. Lim. 2019. "Characterization of Focal EEG Signals: A Review." *Future Generation Computer Systems* 91 (6): 290–299. doi:10.1016/j.future.2018.08.044.

Agarap, A. F. 2018. "Deep Learning Using Rectified Linear Units (Relu)." arXiv preprint arXiv:1803.08375.

Alom, M. Z., Taha, T. M., Yakopcic, C., Westberg, S., Sidike, P., Nasrin, M. S., Van Esesn, et al. 2018. "The History Began from Alexnet: A Comprehensive Survey on Deep Learning Approaches." arXiv preprint arXiv:1803.01164.

Arroyo-Fernández, I., Forest, D., Torres-Moreno, J. M., Carrasco-Ruiz, M., Legeleux, T. and Joannette, K., et al. 2018. "Cyberbullying Detection Task: The Ebsi-Lia-Unam System (Elu) at coling'18 Trac-1." In *Proceedings of the first workshop on trolling, aggression and cyberbullying (TRAC-2018)*, European, August, 140–149.

AswinGopinathan. 30 March 2021. Cyclone, wildfire, flood and Earthquake[eb/ol]. https://www.kaggle.com/aswin1871/cyclonewildfireflood-and-earthquake

Batou, B. 2019. "Wave Dispersion Properties in Imperfect Sigmoid Plates Using Various HSDTs." *Steel and Composite Structures, An International Journal* 33 (5): 699–716.

Cai, J., and Y. Chen. 2022. "A Novel Unsupervised Deep Learning Method for the Generalization of Urban Form." *Geo-Spatial Information Science* 25 (4): 568–587. doi:10.1080/10095020.2022.2068384.

Camero, A., J. Toutouh, and E. Alba. 2019. "A Specialized Evolutionary Strategy Using Mean Absolute Error Random Sampling to Design Recurrent Neural Networks." arXiv preprint arXiv:1909.02425, 1–10.

Chai Q., S. Sun, J. Qiu, M. Chen, Z. Wei, and W. Cong. 2021. "Prediction Method of Power Grid Emergency Supplies Under Meteorological Disaster Conditions." *Journal of Shandong University (Engineering Science)* 51 (3): 76–83. in Chinese.

Chen, C. F., Panda, R. and Fan, Q. 2021. "Regionvit: Regional-To-Local Attention for Vision Transformers." arXiv preprint arXiv:2106.02689.

Chen, Y., and C. Shi. 2019. "Network Revenue Management with Online Inverse Batch Gradient Descent Method." *SSRN Electronic Journal* 2022 (1): 57. doi:10.2139/ssrn.3331939.

Chen, H., Y. Wang, T. Guo, C. Xu, Y. Deng, and Z. Liu 2021. "Pre-Trained Image Processing Transformer." In *Proceedings of the IEEE/CVF Conference on Computer Vision and Pattern Recognition*, Xian, May, 12299–12310.

Chu, X., Tian, Z., Wang, Y., Zhang, B., Ren, H., Wei, X., Xia, H., et al. 2021. "Twins: Revisiting Spatial Attention Design in Vision Transformers." arXiv e-prints, arXiv-2104.

Devlin, J., Chang, M. W., Lee, K., and Toutanova, K. 2018. "Bert: Pre-Training of Deep Bidirectional Transformers for Language Understanding." arXiv preprint arXiv:1810.04805.

Dong, Y., W. Shi, B. Du, X. Hu, and L. Zhang. 2021. "Asymmetric Weighted Logistic Metric Learning for Hyperspectral Target Detection." *IEEE Transactions on Cybernetics* 52 (10): 11093–11106. doi:10.1109/TCYB.2021.3070909.

Dosovitskiy, A., Beyer, L., Kolesnikov, A., Weissenborn, D., Zhai, X., Unterthiner, T., Dehghani, M., et al. 2020. "An Image is Worth 16x16 Words: Transformers for Image Recognition at Scale." arXiv preprint arXiv: 2010.11929.

Du, S., J. Lee, H. Li, and L. Wang 2019. "Gradient Descent Finds Global Minima of Deep Neural Networks." In *International conference on machine learning*, Shanxi, May, 1675–1685.

Eweida, S. M., A. Salem, Y. M. Shaker, N. Samy, I. Yassen, and R. H. Mohamed. 2021. "Vitamin D Levels and Vitamin D Receptor Genetic Variants in Egyptian Cardiovascular Disease Patients with and Without Diabetes." *Egyptian Journal of Medical Human Genetics* 22 (1): 1–12. doi:10.1186/s43042-021-00174-9.

Gao, P., M. Zheng, X. Wang, J. Dai, and H. Li 2021. "Fast Convergence of Detr with Spatially Modulated Co-Attention." In *Proceedings of the IEEE/CVF International Conference on Computer Vision*, The Dominican Republic, November, 3621–3630.

Garcia, J., V. Rodellas, J. Tamborski, M. Diego-Feliu, P. van Beek, Y. Weinstein, M. Charette, et al. 2021. "Radium Isotopes as Submarine Groundwater Discharge (SGD) Tracers: Review and Recommendations." *Earth-Science*

Reviews 220 (8): 103681. doi:10.1016/j.earscirev.2021.103681.

Gupta, D., B. B. Hazarika, and M. Berlin. 2020. "Robust Regularized Extreme Learning Machine with Asymmetric Huber Loss Function." *Neural Computing & Applications* 32 (16): 12971–12998. doi:10.1007/s00521-020-04741-w.

Jamin, A., and A. Humeau-Heurtier. 2019. "(Multiscale) Cross-Entropy Methods: A Review." *Entropy* 22 (1): 45. doi:10.3390/e22010045.

Lee, Y., Hwang, J.W., Lee, S., Bae, Y. and Park, J. 2019. "An Energy and GPU-Computation Efficient Backbone Network for Real-Time Object Detection." In *Proceedings of the IEEE/CVF Conference on Computer Vision and Pattern Recognition Workshops*, USA, June, 1–10.

Lee, H. J., I. Ullah, W. Wan, Y. Gao, and Z. Fang. 2019. "Real-Time Vehicle Make and Model Recognition with the Residual SqueezeNet Architecture." *Sensors* 19 (5): 982. doi:10.3390/s19050982.

Li, D., S. B. Huang, Y. S. Kang, and X. Hunag. 2022. "Micro-Current Technology and Its Application for Prediction of Coal and Rock Dynamic Disasters." *Chinese Journal of Rock Mechanics and Engineering* 41 (4): 764–774. in Chinese.

Li, Y., C. Xu, Z. Chi, and F. Zhang. 2021. "Research on Earthquake Disaster Loss Prediction and Evaluation Based on Softmax Regression Model." *Journal of Hefei University of Technology (Natural Science Edition)* 44 (12): 1676–1681. (in Chinese).

Li, Z., K. Jiang, S. Qin, Y. Zhong, A. Elofsson, A. Schlessinger, and A. Schlessinger. 2021. "GCSENet: A GCN, CNN and SENet Ensemble Model for microRna-Disease Association Prediction." *PLoS Computational Biology* 17 (6): e1009048. doi:10.1371/journal.pcbi.1009048.

Liu, S., Y. -S. Wang, Q. Zhang, Q. Zhou, L. -Z. Cao, C. Jiang, Z. Zhang, N. Yang, Q. Dong, and X. -N. Zuo. 2021. "Chinese Color Nest Project: An Accelerated Longitudinal Brain-Mind Cohort." *Developmental Cognitive Neuroscience* 52 (1): 101020. doi:10.1016/j.dcn.2021.101020.

Lucas, A., S. Lopez-Tapia, R. Molina, and A. K. Katsaggelos. 2019. "Generative Adversarial Networks and Perceptual Losses for Video Super-Resolution." *IEEE Transactions on Image Processing* 28 (7): 3312–3327. doi:10.1109/TIP.2019.2895768.

Luque, A., A. Carrasco, A. Martín, and A. de las Heras. 2019. "The Impact of Class Imbalance in Classification Performance Metrics Based on the Binary Confusion Matrix." *Pattern Recognition* 91 (10): 216–231. doi:10.1016/j.patcog.2019.02.023.

Marques, G., D. Agarwal, and I. de la Torre Díez. 2020. "Automated Medical Diagnosis of COVID-19 Through EfficientNet Convolutional Neural Network." *Applied Soft Computing* 96 (5): 106691. doi:10.1016/j.asoc.2020.106691.

Muehlebach, M., and M. Jordan 2019. "A Dynamical Systems Perspective on Nesterov Acceleration". In *International Conference on Machine Learning*, Shanxi, May, 4656–4662.

Nakajima, K., H. Iwata, Y. Hattori, S. Hashimoto, K. Hayashi, T. Toshito, F. Baba, et al. 2019. "Image-Guided Proton Therapy (IGPT) for Oligometastatic Liver Tumors from Gastric/Colorectal Cancer." *International Journal of Radiation Oncology, Biology, Physics* 105 (1): E224–225. doi:10.1016/j.ijrobp.2019.06.1982.

Ogie, R. I., J. C. Rho, and R. J. Clarke 2018. "Artificial Intelligence in Disaster Risk Communication: A Systematic Literature Review." In *2018 5th International Conference on Information and Communication Technologies for Disaster Management (ICT-DM)*, Cairo, December 1-8.

Qin, X., and Z. Wang 2019. "Nasnet: A Neuron Attention Stage-By-Stage Net for Single Image Deraining." arXiv preprint arXiv:1912.03151.

Rabie, W. B., and H. M. Ahmed. 2021. "Dynamical Solitons and Other Solutions for Nonlinear Biswas–Milovic Equation with Kudryashov's Law by Improved Modified Extended Tanh-Function Method." *Optik* 245 (6): 167665. doi:10.1016/j.ijleo.2021.167665.

Recht, B., Roelofs, R., Schmidt, L., and Shankar, V. 2018. "Do CIFAR-10 Classifiers Generalize to CIFAR-10?." arXiv preprint arXiv:1806.00451.

Rodríguez, E. C. 2019. "Total Knee Arthroplasty Using Hinge Joints: Indications and Results." *EFORT Open Reviews* 4 (4): 121–132. doi:10.1302/2058-5241.4.180056.

Singla, S., Singla, S. and Feizi, S. 2021. "Improved Deterministic L2 Robustness on CIFAR-10 and CIFAR-100." In *International Conference on Learning Representations*, Vancouver, September, arXiv preprint arXiv:2108.04062.

Song, Y. S., and M. J. Park. 2019. "Development of Damage Prediction Formula for Natural Disasters Considering Economic Indicators." *Sustainability* 11 (3): 868. doi:10.3390/su11030868.

Tan, M., Chen, B., Pang, R., Vasudevan, V., Sandler, M., Howard, A. and Le, Q. V. 2019. "Mnasnet: Platform-Aware Neural Architecture Search for Mobile." In *Proceedings of the IEEE/CVF Conference on Computer Vision and Pattern Recognition*, United States, June, 2820–2828.

Tan, M., and Q. V. Le 2019. "Mixconv: Mixed Depthwise Convolutional Kernels." arXiv preprint arXiv:1907.09595.

Wang, W., Yao, L., Chen, L., Lin, B., Cai, D., He, X. and Liu, W. 2021. "Crossformer: A Versatile Vision Transformer Based on Cross-Scale Attention." arXiv e-prints, arXiv-2108.

Ward, R., Wu, X. and Bottou, L. 2019. "Adagrad Stepsizes: Sharp Convergence Over Nonconvex Landscapes." In *International Conference on Machine Learning*, Shanxi, May, 6677–6686.

Wen, L., X. Li, and L. Gao. 2020. "A Transfer Convolutional Neural Network for Fault Diagnosis Based on ResNet-50." *Neural Computing & Applications* 32 (10): 6111–6124. doi:10.1007/s00521-019-04097-w.

Wu, C, W. Xiang, and L. Han. 2022. "Machine Learning Disaster Prediction Method Based on Subway Construction Accident Cases." *Practice and Understanding of Mathematics* 52 (1): 92–102. (in Chinese).

Xu, X., J. Li, Y. Yang, and F. Shen. 2020. "Toward Effective Intrusion Detection Using Log-Cosh Conditional Variational Autoencoder." *IEEE Internet of Things Journal* 8 (8): 6187–6196. doi:10.1109/JIOT.2020.3034621.

Yang, L., and H. Dong. 2019. "Robust Support Vector Machine with Generalized Quantile Loss for Classification and Regression." *Applied Soft Computing* 81 (20): 105483. doi:10.1016/j.asoc.2019.105483.

Zhang, H., G. Han, X. Ma, S. Li, H. Xu, T. Shi, J. Yuan, et al. 2023. "Spectral Energy Model-Driven Inversion of XCO2 in IPDA Lidar Remote Sensing." *IEEE Transactions on Geoscience and Remote Sensing* 61 (25): 1–9. doi:10.1109/TGRS.2023.3238117.

Zhang, H., and H. Zhang. 2022. "LungSeek: 3D Selective Kernel Residual Network for Pulmonary Nodule Diagnosis." *The Visual Computer* 2023 (39): 1–14. doi:10.1007/s00371-021-02366-1.

Zhang, J., H. Zhao, A. Yao, Y. Chen, and L. Zhang 2018. "Efficient Semantic Scene Completion Network with Spatial Group Convolution." In *Proceedings of the European Conference on Computer Vision (ECCV)*, Munich, September, 733–749.

Zhao, Y., X. Ni, Y. Ding, and Q. Ke 2018. "Paragraph-Level Neural Question Generation with Maxout Pointer and Gated Self-Attention Networks." In *Proceedings of the 2018 Conference on Empirical Methods in Natural Language Processing*, Belgium, October, 3901–3910.

Zhao, C., R. Shuai, L. Ma, W. Liu, and M. Wu. 2022. "Improving Cervical Cancer Classification with Imbalanced Datasets Combining Taming Transformers with T2T-ViT." *Multimedia Tools and Applications* 81 (17): 24265–24300. doi:10.1007/s11042-022-12670-0.

Zhuang, J., Tang, T., Ding, Y., Tatikonda, S. C., Dvornek, N., Papademetris, X. and Duncan, J. 2020. "Adabelief Optimizer: Adapting Stepsizes by the Belief in Observed Gradients." *Advances in Neural Information Processing Systems* 33 (1): 18795–18806.

Zou, Y., L. Zhao, S. Qin, M. Pan, and Z. Li 2020. "Ship Target Detection and Identification Based on Ssd_mobilenetv2." In *2020 IEEE 5th Information Technology and Mechatronics Engineering Conference (ITOEC)*, Shanghai, June, 1676–1680.